Characterization of filter materials for single-shot dual-energy imaging

Junwoo Kim [a], Dong Woon Kim [a], Jinwoo Kim [a], Junbeom Park [a], Ho Kyung Kim [a,b*]
[a]*School of Mechanical Engineering, Pusan National University, Busan 46241, Republic of Korea*
[b]*Center for Advanced Medical Engineering, Pusan National University, Busan 46241, Republic of Korea*
[*]*Corresponding author: hokyung@pusan.ac.kr*

1. Introduction

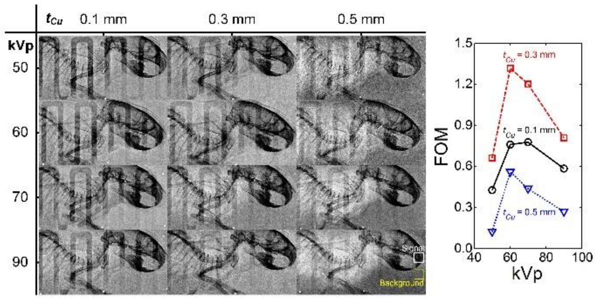

Fig. 1. Bone-enhanced DE images obtained for a postmortem mouse using the sandwich detector for various combinations of kVp and t_{Cu}.

We previously described the sandwich configuration detector by stacking two flat-panel detectors (FPDs) and demonstrated its prospect for “motion-artifact-free” single-shot dual-energy (DE) imaging by obtaining bone and soft-tissues images of a postmortem mouse [1, 2]. The two FPDs used the same CMOS photodiode arrays but the scintillators with different thicknesses: the thicker one for the rear FPD to achieve high quantum efficiency with the higher-energy x-ray spectrum. An intermediate copper filter was used to further increase energy separation between the two FPDs. According to another previous study, bone-enhanced DE images were obtained for a postmortem mouse using the sandwich detector for various combinations of kVp and t_{Cu}. The DE images were obtained by using weighted logarithmic subtraction of two images obtained from the front- and rear- detector. For the maxillary bone and neighboring background regions, the figure of merits (FOM) were calculated using Eq. 1, and the results are shown in figure 1.

2. Materials and Methods

2.1 Sandwich detector

The sandwich detector consisted of FPDs and intermediate filter for various materials and thickness. The FPDs used the same photodiode array (RadEye1TM, Teledyne Rad-icon Imaging Corp., Sunnyvale, CA) and gadolinium oxysulfide (Gd2O2S : Tb) phosphor screens (Carestream Health Inc., Rochester, NY) with different thickness: thinner (~ 34 mg cm-2) for the front and thicker (~ 67 mg cm-2) for the rear detector layers, respectively. The photodiode array had 0.048 mm-sized pixels arranged in 512 × 1024 format.

2.2 Fourier performance

The detective quantum efficiency (DQE) of the jth detector layer (j designates F or R for front or rear detector, respectively) is given by

$$\mathrm{DQE}_j(u) = \frac{\bar{q}_{in} G_j^2 \mathrm{MTF}_j^2(u)}{\mathrm{NPS}_j(u)} = \frac{\mathrm{MTF}_j^2}{\bar{q}_{in}\left[\mathrm{NPS}_j(u)/\bar{d}_j^2\right]},$$

where $\bar{q}$ (mm^2) denotes the average incident photon fluence. G (DN mm^2) is the detector gain relating $\bar{q}$ to the average pixel signal $\bar{d}$ in units of digital number (DN).
We measure the modulation-transfer function (MTF), noise-power spectrum (NPS), and DQE of each detector layer of the sandwich detector for various tube voltages, materials and thicknesses of an intermediate filter.

2.3 Cascaded-system analysis

In a previous study, we showed the cascaded model describing the signal and noise from each detector layer in the sandwich detector [6]. Similar to Fourier performance, we can describe the DQE of the j th detector layer of the sandwich detector in cascaded-system analysis model as follows:

$$\mathrm{DQE}_j(u) = \frac{\mathrm{MTF}_j^2(u)}{\bar{q}_{in}\left[W'_{j,\mathrm{indirect}}(u) + W'_{j,\mathrm{direct}}(u) + W'_{j,\mathrm{add}}(u)\right]}.$$

To investigate spectral energy separation for various filter materials in the sandwich detector. We may construct the FOM in the single-shot DE images using Eq 4.

$$\mathrm{FOM}_j = C_j^2 A_{eff} \bar{q}_0 \left[\frac{\omega_j^2}{\mathrm{DQE}^F(0)} + \frac{1}{\mathrm{DQE}^R(0)}\right]^{-1}.$$

3. Preliminary results

Figure 2(a) shows incident x-ray spectra for rear in the sandwich detector after transmitted the front detector and various filter materials. The spectra transmitted through the various filter materials all have a transmittance of ~ 30 %. Then, filter thickness are Cu = ~ 0.18 mm, Mo = ~ 0.06 mm, Gd = ~ 0.13 mm, Sn = ~ 0.07 mm, respectively.

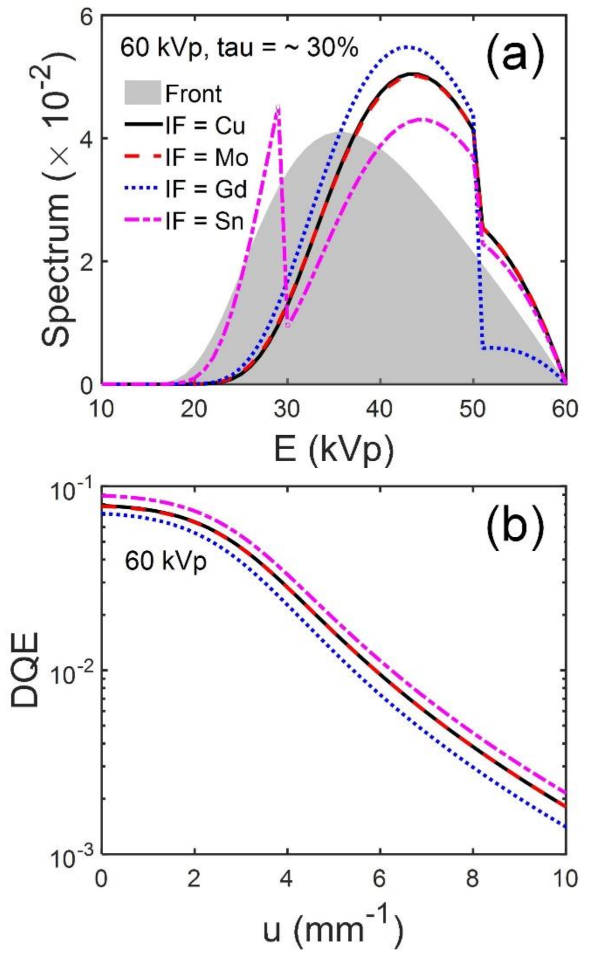

Fig. 2. (a) Spectra after transmission front detector and various intermediate filter with tau = ~ 30 %. (b) Spatial-frequency-dependent DQE with 60 kVp, ~ 20 mR.

Figure 2(b) is spatial-frequency-dependent DQE of the rear detector layer at 60 kVp, ~ 20 mR with filter materials.

4. Further study

The remained further study before the meeting includes the followings:

- the quantitative analysis of the measured MTF, NPS, and DQE characteristics for various intermediate filter with the helps from the developed model or simulations;
- the quantitative analysis of the correlated or K-fluorescence x-ray generated from various filter materials;
- quantitatively analysis of the single-shot dual-energy imaging for various filter materials;

Acknowledgments

This work was supported by the National Research Foundation of Korea (NRF) grant funded by the Korean government (MSIP) (No. 2017M2A2A6A01019930).

REFERENCES

[1] J. C. Han, H. K. Kim, D. W. Kim, S. Yun, H. Youn, S. Kam, J. Tanguay, and I. A. Cunningham, Single-shot dual-energy x-ray imaging with a flat-panel sandwich detector for preclinical imaging, Cur. Appl. Phys., Vol.14, No.12, pp. 1734–1742, 2014.

[2] S. Yun, J. C. Han, D. W. Kim, H. Youn, H. K. Kim, S. Tanguay, and I. A. Cunningham, Feasibility of active sandwich detectors for single-shot dual-energy imaging, in Proc. SPIE, 9033, pp. 90335T, 2014.

[3] J. Kim, D. Kim, S. Kam, E. Park, H. Youn, and H. K. Kim, Effects of the energy-separation filter on the performance of each detector layer in the sandwich detector for single-shot dual-energy imaging, J. Instrum., Vol.11, No.2, pp. C02065, 2016.

[4] R. E. Alvarez, J. A. Seibert, and S. K. Thompson, Comparison of dual energy detector system performance, Med. Phys., Vol.31, No.3, pp. 556–565, 2004.

[5] S. Richard and J. H. Siewerdsen, Optimization of dual-energy imaging systems using generalized NEQ and imaging task, Med. Phys., Vol.34, No.1, pp. 127–139, 2007.

[6] D. W. Kim, H. K. Kim, H. Youn, S. Yun, J. C. Han, J. Kim, S. Kam, J. Tanguay, and I. A. Cunningham, Signal and noise analysis of flat-panel sandwich detectors for single-shot dual-energy x-ray imaging, in Proc. SPIE, 9412, pp. 94124A, 2015.